3-Hydroxy-3-methylglutaryl-CoA Synthase: Participation of Invariant Acidic Residues in Formation of the Acetyl-S-Enzyme Reaction Intermediate[‡]

Kelly Y. Chun, Dmitriy A. Vinarov, and Henry M. Miziorko*

Department of Biochemistry, Medical College of Wisconsin, Milwaukee, Wisconsin 53226

Received August 1, 2000; Revised Manuscript Received September 22, 2000

ABSTRACT: Inactivation of HMG-CoA synthase by a carboxyl-directed reagent, 1-ethyl-3-(3-dimethylaminopropyl)carbodiimide (EDC), in a concentration-dependent and substrate-protectable manner suggested that the active site contains reactive acidic amino acids. This observation prompted functional evaluation of 11 invariant acidic amino acids by site-directed mutagenesis. Characterization of the isolated synthase variants' ability to catalyze overall and partial reactions identified three mutant synthases (D99A, D159A, and D203A) that exhibit significant diminution of k_{cat} for the overall reaction (10^2-, 10^3-, and 10^4-fold decreases, respectively). D99A, D159A, and D203A form the acetyl-S-enzyme intermediate very slowly (0.0025, 0.0026, 0.0015 U/mg, respectively, measured at pH 7.0 and 22 °C) as compared to the wild-type synthase (1.59 U/mg), where intermediate formation approaches rate-limiting status. Differences in substrate saturation do not account for impaired activities or rates of intermediate formation. The structural integrity of the purified mutants' active sites is demonstrated by their abilities to bind a spin-labeled acyl-CoA analogue (R·CoA) with affinities and stoichiometries comparable to values measured for wild-type synthase. The impact of three distinct amino acids on reaction intermediate formation supports a mechanism of acetyl-S-enzyme formation that probably requires formation and directed collapse of a tetrahedral adduct. ^{18}O-induced shift of the ^{13}C NMR signal of ^{13}C acetyl-S-enzyme demonstrates that an analogous tetrahedral species is produced upon solvent exchange with the acetyl-S-enzyme. Partial discrimination between the functions of D99, D159, and D203 becomes possible based on the observation that D159A and D203A synthases exhibit retarded kinetics of solvent ^{18}O exchange while D99A fails to support ^{18}O exchange.

3-Hydroxy-3-methylglutaryl-CoA (HMG-CoA)[1] synthase catalyzes the production of a key intermediate in cholesterogenic and ketogenic pathways by a reaction that may be described as a three-step process (*1*), as shown in Scheme 1. The cholesterogenic isoform has been isolated from cytosol (*2*), and the ketogenic isoform has been isolated from mitochondria (*3*); these are encoded by distinct genes (*4*, *5*). The enzyme catalyzes a functionally irreversible reaction and may be viewed as a committed step for both cholesterogenic and ketogenic pathways. As such, it is not surprising that HMG-CoA synthase activity is regulated, with each isoform subject to a different type of transcriptional control (*6*, *7*), and the mitochondrial isoform sensitive to inhibition by succinyl-CoA (*8*). Recently, it has been demonstrated that deficiency of the mitochondrial isoform correlates with human metabolic disease (*9*). Moreover, the cytosolic isoform has been identified as a potentially useful target for drugs aimed at lowering cholesterol levels.

Scheme 1: Reactions Catalyzed by HMG-CoA Synthase

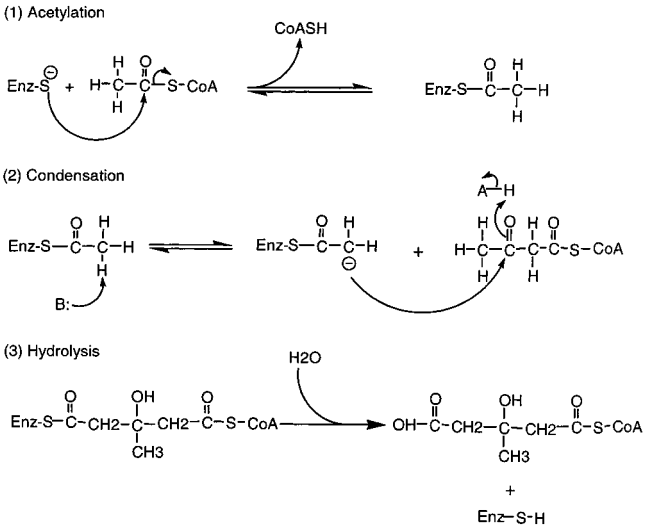

Early mechanistic and protein chemistry studies on the avian mitochondrial isoform led to selective modification (*10*) and mapping (*11*) of the cysteine residue that forms the acetyl-S-enzyme reaction intermediate. Development of a recombinant form of the avian cytosolic enzyme (*12*) allowed the demonstration of an absolute requirement for cysteine-129 in formation of the acetyl-S-enzyme reaction intermediate. This residue remains invariant in all available deduced HMG-CoA sequences, and the flanking region is highly conserved. Evaluation of invariant histidine residues led to the identification of a residue (histidine-264) that

[†] This work was supported, in part, by a research grant from the National Institutes of Health (DK21491) to H.M.M. K.Y.C. is an American Heart Association predoctoral fellow. D.A.V. is an American Heart Association postdoctoral fellow.

* To whom correspondence should be addressed. Telephone: (414)456-8437. Fax: (414)456-6570. E-mail: miziorko@mcw.edu.

[1] Abbreviations: HMG-CoA, 3-hydroxy-3-methylglutaryl-CoA; R·CoA, 3-carboxy-2,2,5,5-tetramethyl-1-pyrrolidinyloxyl-CoA; EDC, 1-ethyl-3-(3-dimethylaminopropyl)carbodiimide.

10.1021/bi001805m CCC: $19.00
Published on Web 11/02/2000

anchors binding of the second substrate, acetoacetyl-CoA (*13*).

Identification of additional residues that directly support reaction chemistry has been impaired by the presence of highly reactive cysteine residues (*14*), which result in a multiplicity of modification sites upon pursuit of a traditional affinity labeling approach. With the recent increase in deduced primary sequences for HMG-CoA synthase from a wider variety of organisms, it has now become practical to screen for classes of hyperreactive side chains and to test the function of invariant residues that contain these functional groups. This paper describes the utility of this combined approach in detecting several acidic amino acids important for formation of HMG-CoA synthase's acetyl-S-enzyme reaction intermediate.

EXPERIMENTAL PROCEDURES

Materials

Escherichia coli BL21 (DE3) and the expression vector pET-3d were purchased from Novagen (Madison, WI). *E.coli* strain DH5α was obtained from Bethesda Research Laboratory (Gaithersburg, MD). Deoxyoligonucleotides were purchased from Operon (Alameda, CA). Qiagen (Chatsworth, CA) plasmid kits were used to isolate plasmid DNA from bacterial cultures. Qiaex (Qiagen Inc.) reagents and protocols were used for extraction of nucleic acid fragments from agarose gels. The restriction enzymes and T4 DNA ligase were purchased from New England Biolabs (Beverly, MA) and Amersham Pharmacia Biotech, Inc (Piscataway, NJ). *Pfu* DNA polymerase was obtained from Stratagene (LaJolla, CA). DNA sequencing was performed using an ALF automated sequencer; the cyclosequencing kit and protocol were provided by Amersham Pharmacia Biotech, Inc. (Piscataway, NJ). Ampicillin and isopropyl-β-D-thiogalactoside were purchased from United States Biochemical (Cleveland, OH). [1-^{14}C]acetyl-CoA was purchased from Moravek Biochemical (Brea, CA). Unlabeled and ^{13}C-enriched acetyl-CoA were prepared from the appropriate acetic anhydride. Acetoacetyl-CoA was similarly prepared with diketene replacing the anhydride. All other reagents were purchased from Sigma (St. Louis, MO), Aldrich (Milwaukee, WI), Pharmacia Biotech, Inc. (Piscataway, NJ) or Bio-Rad (Richmond, CA).

Methods

Construction of HMG-CoA Synthase Mutants: Overlap Extension PCR Mutagenesis. Point mutations were engineered in HMG-CoA synthase encoding cDNA by using the overlap extension PCR technique (*15*) described previously (*13*). Each of the invariant glutamates and aspartates was individually replaced by an alanine. At positions 37 and 63, glutamate was also replaced by glutamine, and at position 64, aspartate was also replaced by asparagine. The following primers were used for introducing the site-specific mutations in the generation of PCR-amplified mutagenic fragments: *E37A*: 5′-AG ACT GAG CTG G***C***G AAG TAT GAC GG-3′and 5′-CC GTC ATA CTT C***G***C CAG CTC AGT CT-3′; *E37Q*: 5′-AG ACT GAG CTG ***C***AG AAG TAT GAC GG-3′and 5′-CC GTC ATA CTT CT***G*** CAG CTC AGT CT-3′; *E63A*: 5′-GC TCT GAC CGA G***C***G GAT ATC AAT TC-3′and 5′-GA ATT GAT ATC C***G***C TCG GTC AGA GC-3′; *E63Q*: 5′-GC TCT GAC CGA ***C***AG GAT ATC AAT TC-3′and 5′-GA ATT GAT ATC CT***G*** TCG GTC AGA GC-3′; *D64A*: 5′-CT GAC CGA GAG G***C***T ATC AAT TCC CT-3′ and 5′-AG GGA ATT GAT A***G***C CTC TCG GTC AG-3′; *D64N*: 5′-CT GAC CGA GAG ***A***AT ATC AAT TCC CT-3′ and 5′-AG GGA ATT GAT AT***T*** CTC TCG GTC AG-3′; *E95A*: 5′-C TGA CCG AGA GA***A*** TAT CAA TTC CCT-3′ and 5′-AGG GAA TTG ATA ***T***TC TCT CGG TCA G-3′; *D99A*: 5′-CA ATA ATT G***C***T AAA TCA AAA-3′ and 5′-TTT TGA TTT A***G***C AAT TAT TG-3′; *E212A*: 5′-ACA GAT GTA G***CG*** GGA ATT GAC-3′and 5′-GTC AAT TCC ***CG***C TAC ATC TGT-3′; *D124A*: 5′-GAA GGA ATT G***C***C ACA ACC AAT G-3′ and 5′-C ATT GGT TCT G***G***C AAT TCC TTC-3′; *D159A*: 5′-TT GCT GGA G***C***C ATT GCT GTG-3′and 5′-CAC AGC AAT G***G***C TCC AGC AA-3′; *D203A*: 5′-AT GCT TAT G***G***C TTC TAT AAA-3′and 5′-TTT ATA GAA G***G***C ATA AGC AT-3′; *D217A*: 5′-CT GTA GTT G***C***T GGC AAA CTG-3′and 5′-CAG TTT GCC A***G***C AAC TAC AG-3′; *D282A*: 5′-G TTG CTG AAT G***C***C TTT CTC AG-3′and 5′-CT GAG AAA G***G***C ATT CAG CAA C-3′. The boldfaced and italicized characters indicate the base changes that were made to generate mutagenic codons. Mutagenesis was carried out by PCR using P*fu* DNA polymerase according to the manufacturer's protocol. The amplification procedure included 25 cycles of denaturation (95 °C, 1 min), annealing (50 °C, 40 s), and extension (70 °C, 40−60 s) followed by a cycle of extension at 72 °C for 5 min. The fragment encoding the mutation was isolated by gel electrophoresis and purified using Qiaex. The product was digested with appropriate restriction endonucleases, and the resulting fragment was purified by gel electrophoresis. The expression plasmid was prepared by ligation of the mutagenic fragment with the remainder of the coding sequence and vector, isolated from wild-type expression plasmid. The ligation mixture was used to transform competent DH5α cells. Mutagenic plasmid DNA was isolated from selected transformants and analyzed by restriction mapping and DNA sequencing. The verified plasmids were transformed into competent BL21(DE3) cells for subsequent expression of mutant synthase enzymes.

Isolation of HMG-CoA Synthase Mutants. The procedure (*12*) developed for purification of the wild-type enzyme was followed for isolation of the mutant enzymes from 2-L bacterial cultures. Protein content of the purified enzymes was estimated by the Bradford assay (*16*), using bovine serum albumin as the standard. The purity of the enzymes was assessed by densitometry measurements of bands on SDS−polyacrylamide gels.

Measurement of the Overall Condensation Reaction. A standard spectrophotometric assay (*2, 12*) was employed to generate the initial velocity data needed for estimation of K_m for acetyl-CoA for mutants D99A and D159A. The reaction mixture included 100 mM Tris-HCl, pH 8.2, 100 μM EDTA, appropriately diluted HMG-CoA synthase (approximately 6 μg for wild-type enzyme), 20 μM acetoacetyl-CoA, and various concentrations of acetyl-CoA (1 μM−1 mM). The reaction rate at 30 °C was monitored by acetyl-CoA-dependent loss of absorbance at 300 nm, due to depletion of the enolate of acetoacetyl-CoA. For estimation of K_m for acetoacetyl-CoA, 40 mM magnesium chloride was added to the assay mixture to afford a 5-fold improvement

in sensitivity: the millimolar extinction coefficient (300 nm) increased from 3.6 to 18.0 under these conditions. K_m for acetoacetyl-CoA was measured in the presence of constant acetyl-CoA (200 μM) and varied concentrations (0.3−110 μM) of acetoacetyl-CoA.

When improved sensitivity was required, the overall reaction rate of catalytically impaired mutant synthases was measured using the equivalent radioisotopic assay (*2*). The reaction mixture contained 100 mM Tris-HCl, pH 8.2, 100 μM EDTA, 20 μM acetoacetyl-CoA, varied concentrations of [^{14}C]acetyl-CoA (8000−12000 dpm/nmol), and appropriately diluted mutant synthase enzyme. The reaction was initiated by addition of radiolabeled acetyl-CoA to the assay mixture containing the rest of the components at 30 °C. At specified time intervals, 40-μL aliquots were removed from the incubation mixture and acidified with 6 N HCl. The mixture was heated to dryness, and acid-stable radioactivity due to [^{14}C]HMG-CoA formation was measured by liquid scintillation counting.

All tabulated kinetic parameters derive from nonlinear regression fits of the experimental rate data (Grafit program; Erithacus software); reported errors reflect the quality of these computer fits to a series of data points.

EPR Measurements of Spin-Labeled Acyl-CoA Binding. Measurement of R·CoA binding by EPR was performed using a Varian Century-Line 9 GHz spectrometer. Samples used for recording of conventional X-band EPR spectra contained a variable concentration of HMG-CoA synthase sites (10−300 μM) in 50 mM sodium phosphate buffer, pH 7.0, and a fixed concentration of R·CoA (25 μM). The spectra were recorded at ambient temperature with modulation amplitude of 1 G, modulation frequency of 100 kHz, and microwave power of 5 mW. Field sweep was 100 G, and time constant was 0.5 s. R·CoA bound to HMG-CoA synthase was calculated by comparing the amplitudes of high field lines of sample spectra with the corresponding lines observed for a solution containing an equal concentration of R·CoA in a buffer. Under the instrument gain and modulation amplitude conditions used to obtain these spectra, only unbound R·CoA produces a signal (*17*). Therefore, the fraction of R·CoA free in each sample was calculated by dividing the amplitude of the spectral line measured in the protein containing samples by the amplitude of the signal measured in the absence of protein; $[R{\cdot}CoA]_{bound} = ([R{\cdot}CoA]_{total} - [R{\cdot}CoA]_{free})$. A Scatchard plot, fit by linear regression, was used to determine the binding constants and binding stoichiometry of R·CoA to both wild-type and mutant synthases. K_d was calculated on the basis of three separate experiments. The EPR spectra of bound R·CoA were obtained at 5 G modulation amplitude and variable gain.

Measurement of Acetyl-CoA Binding. Binding of radiolabeled substrate to enzyme was determined by a modification of the procedure of Vollmer et al. (*18*). After a 5-min incubation of the enzyme (150 μg) in 100 mM sodium phosphate, pH 7.0 at 30 °C, the incubation mixture was placed on ice. [^{14}C]Acetyl-CoA (11500 dpm/nmol) was added to bring the 100-μL reaction mixture to a final concentration of 200−1000 μM. Unbound acetyl-CoA was removed using a G-50 centrifugal column equilibrated with 20 mM sodium phosphate, pH 7.0 at 4 °C. Protein-bound radioactivity was determined by liquid scintillation counting.

Determination of the Stoichiometry of Covalent Acetylation. Modification of the procedures described by Miziorko et al. (*19*) was performed to determine the stoichiometry of acetyl-S-enzyme. Enzyme (40 μg) in a 0.1-mL incubation mixture (100 mM sodium phosphate buffer, pH 7.0, [1-^{14}C]acetyl-CoA (500 μM−1 mM, 8000−12000 dpm/nmol)) was treated with 1 mL of ice-cold 10% trichloroacetic acid. The denatured protein was transferred to a glass fiber filter, washed extensively with ice-cold 10% trichloroacetic acid and 50 mm sodium pyrophosphate in 500 mM HCl and once with cold absolute ethanol. Filters were dried, and radioactivity was determined by liquid scintillation counting.

Single Condensation Turnover Assay. The reaction was measured by combining several techniques described above. Enzyme (150 μg) was incubated with a saturating concentration of [1-^{14}C]acetyl-CoA (500−1000 μM, 12000 dpm/nmol). The incubation mixture was spun through a 2-mL G-50 size exclusion centrifugal column to remove the unbound acetyl-CoA. Approximately 10-fold excess (over enzyme sites) of unlabeled second substrate (acetoacetyl-CoA) was added to the acetyl-enzyme intermediate recovered in the filtrate to drive the reaction to completion. At specified times, 30-μL aliquots of this reaction mix were removed from the incubation mixture and acidified with 6 N HCl. The mixture was heated to dryness, and acid-stable radioactivity due to condensation product [^{14}C]-HMG-CoA was measured by liquid scintillation counting. At each time point, additional 30-μL aliquots were treated with 1 mL of ice-cold 10% trichloroacetic acid. The denatured protein was transferred to a glass fiber filter, washed extensively with ice-cold 10% trichloroacetic acid and 50 mM sodium phosphate in 500 mm HCl and once with absolute ethanol. Filters were dried, and radioactivity was determined by liquid scintillation counting.

Kinetics of Acetyl-S-Enzyme Intermediate Formation. For the measurement of initial velocity for wild-type enzyme, an Update Instrument ram and model 725 controller were used. Wild-type enzyme (40−200 μg used for the various time points) and various concentrations of [^{14}C]acetyl-CoA were separately placed in syringes A or B. After being rapidly mixed, the sample of enzyme and radiolabeled acetyl-CoA was allowed to react in the delay hose for 25−160 ms prior to mixing and denaturation with trichloroacetic acid (final concentration of 10%). The denatured protein was transferred to a glass fiber filter, washed extensively with ice-cold 10% trichloroacetic acid and 50 mm sodium pyrophosphate in 500 mM HCl and once with cold absolute ethanol. Filters were dried, and radioactivity was determined by liquid scintillation counting. Measurement of rates as a function of [acetyl-CoA] allowed calculation of V_m for intermediate formation.

For the rate measurements of the mutant enzymes (D99A, D159A, and D203A), manual mixing and incubation was performed. Aliquots containing 40 μg of mutant enzymes in incubation mixture (100 mM sodium phosphate buffer, pH 7.0, and various concentrations of [^{14}C]acetyl-CoA (5−2000 μM, 9000 dpm/nmol)) were removed and treated with 1 mL of ice-cold 10% trichloroacetic acid at indicated times. The denatured protein was transferred to a glass fiber filter and washed as described previously. Rate measurements at a series of acetyl-CoA concentrations were computer fit to generate V_m estimates.

Steady-State Assay of Acetyl-CoA Hydrolase Activity. Rates for wild-type and mutant synthases were measured as reported previously (*19*) by monitoring enzyme dependent depletion of [^{14}C]acetyl-CoA after conversion of residual substrate to acid stable [^{14}C]citrate, using excess citrate synthase and oxaloacetate.

Hydrolysis of the Isolated Acetyl-S-Enzyme Reaction Intermediate. Wild-type or mutant enzyme (150 μg, 1.5 mg/mL) in 100 mM sodium phosphate, pH 7.0, was preincubated at 30 °C for 5 min. Acetylation was initiated by adding [1-^{14}C]acetyl-CoA to the preincubation mixture to final concentration of 500−1000 μM. Optimal incubation time required to form the acetyl-S-enzyme intermediate (>0.5 acetyl group/enzyme site) for each mutant and wild-type enzyme was empirically determined: wild type, <5 s; D99A, 22 min; D159A, 18 min; D203A, 35 min. After the specified incubation time, the reaction mixture was passed through a G-50 size exclusion centrifugal column to remove unbound acetyl-CoA. The hydrolysis of the acetyl moiety from the acetyl-S-enzyme intermediate was followed by removing 40-μL aliquots of gel-filtered reaction mixture over time (30 °C) and precipitating the protein-bound radioactivity with 1 mL of ice-cold 10% trichloroacetic acid. The denatured protein was transferred to a glass fiber filter, washed extensively with ice-cold 10% trichloroacetic acid and 50 mm sodium pyrophosphate in 500 mM HCl and once with cold absolute ethanol. Filters were dried, and radioactivity due to covalent acetylation was determined by liquid scintillation counting. Typical initial stoichiometry of acetyl-S-enzyme was 0.6 ± 0.15 (set as 100%). At each time point, the measured acetylation stoichiometry was divided by the initial stoichiometry value to determine percent of acetyl-S-enzyme species remaining. Calculated percent of acetyl-S-enzyme was plotted vs time on a semilog graph to determine $t_{1/2}$ and k (s^{-1}).

^{13}C NMR Measurements. ^{13}C NMR (proton-decoupled) experiments were performed using a Bruker AC-300 instrument operating at 75.469 MHz for ^{13}C. All spectra were recorded at 21 °C. All reported chemical shifts were referenced to TMS. A sweep width of 16000 Hz was used, and 16K data points collected. Signal acquisition employed a 35-deg pulse angle and a 2-s delay between transients. A typical spectrum of ^{13}C-enriched acetyl-CoA, measured in samples with a 2:1 substrate/enzyme site ratio, required 1.5−5 h of data collection (1500−5000 transients). HMG-CoA synthases were exchanged into 10 mM sodium phosphate buffer, pH 7.0, using Centricon-25 membrane cones. After concentration to a site concentration of about 1 mM, the samples were lyophilized and dissolved (without significant loss of activity) in an appropriate volume of either deionized water supplemented with 10% D_2O for internal lock or $H_2{}^{18}O$ supplemented with 10% D_2O for internal lock prior to running the spectra. Two independently exchanged samples were run consecutively, allowing calculation of a standard error for differential isotope shift values. For spectra shown in the figures, the collected data were zero-filled to 64K points and then processed with 5 Hz line broadening to improve signal-to-noise.

RESULTS

Inactivation of HMG-CoA Synthase by a Carboxyl-Directed Reagent. 1-Ethyl-3-(3-dimethylaminopropyl)carbodiimide (EDC), a soluble reagent commonly used to modify acidic amino acids (*20*), inhibits HMG-CoA synthase in a time- and concentration-dependent fashion (Figure 1). Significantly, the loss of activity, which follows first-order kinetics (at 50 μM EDC, $t_{1/2}$ = 13 min), can be retarded by inclusion of the tight-binding substrate, acetoacetyl-CoA, in the incubation mix (at 50 μM EDC + 100 μM acetoacetyl-CoA, $t_{1/2}$ = 35 min). These observations suggest that EDC acts to covalently modify acidic residue(s) within HMG-CoA synthase, including a target within the active site. On this basis, it seemed reasonable to test whether invariant acidic residues are important to the catalytic function of HMG-CoA synthase.

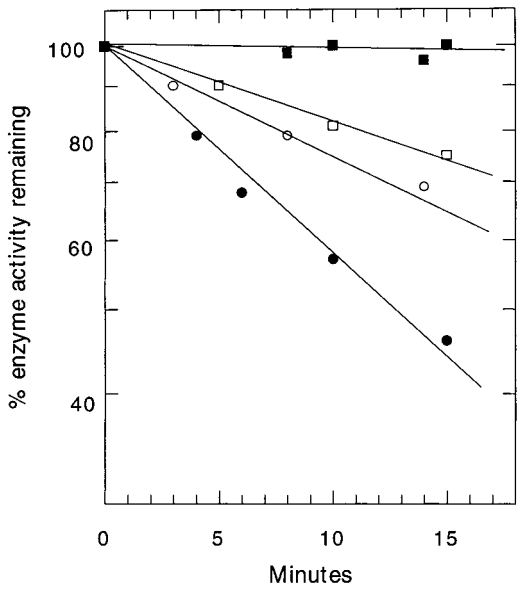

FIGURE 1: *N*-(Dimethylaminopropyl)-*N*′-ethylcarbodiimide (EDC) inactivation of HMG-CoA synthase. Reaction mixtures (100 μL) were prepared containing Tris buffer, pH 5.88 (20 mM), glycine ethyl ester (20mM), HMG-CoA synthase (83 μg), and 0 (■), 20 (○), 50 (●), and 50mM EDC plus 100 μM acetoacetyl-CoA (□). Incubations were initiated by addition of EDC and were performed at 30 °C. Aliquots were withdrawn at the times indicated and assayed for enzyme activity by standard spectrophotometric procedures.

Strategy for Identification of Targets for Mutagenesis. cDNAs encoding cytosolic avian (*5*) and human (*21*) HMG-CoA synthases have been functionally expressed. In addition, over a dozen other eukaryotic cDNA sequences have been reported and assigned as HMG-CoA synthases, based largely on a highly conserved "signature" sequence region that flanks the cysteine which we demonstrated to be the site of formation of the acetyl-S-enzyme reaction intermediate (*11*). Alignment of the deduced eukaryotic sequences indicates 11 invariant aspartate and glutamate residues. Two deduced prokaryotic sequences [from *Borrelia burgdorferi* (*22*) and *Methanobacterium thermoautotrophicum* (*23*)] have also been proposed to represent HMG-CoA synthases. Overall, these prokaryotic proteins exhibit much lower homology (<30%) to human and avian HMG-CoA synthases than observed for sequences from more distantly related eukaryotes such as plants and yeasts (>50%). If the functional assignments offered for these prokaryotic proteins is correct, inclusion of their sequences into an alignment (Figure 2) reduces the number of absolutely invariant acidic residues to five (E63, D64, E95, D159, and D203). A sixth residue

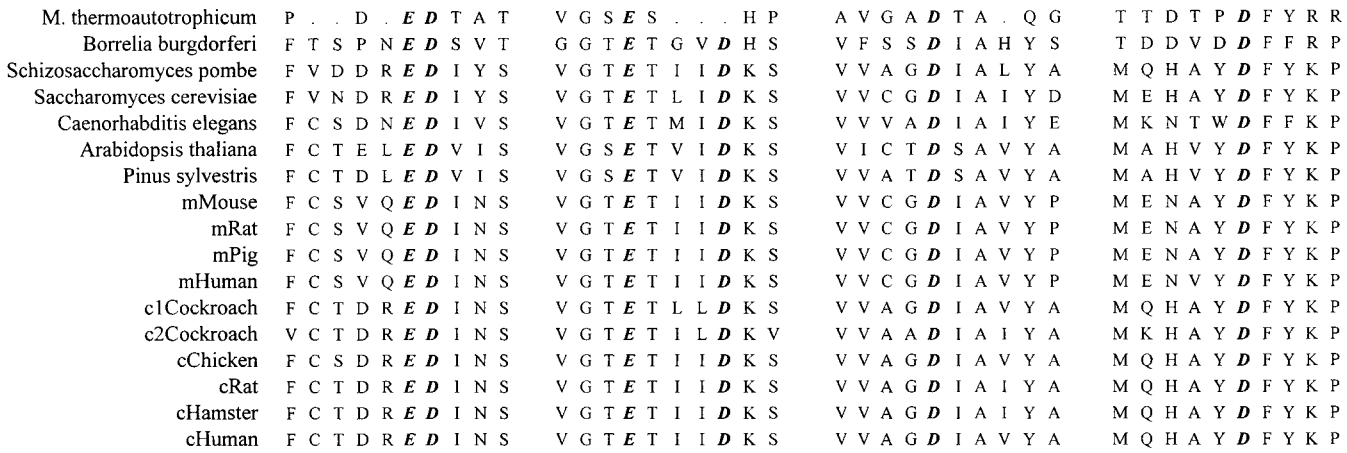

FIGURE 2: Alignment of deduced amino acid sequences for HMG-CoA synthases to indicate the locations of mutated aspartic and glutamic acids. All full-length HMG-CoA synthase sequences were obtained from public databases. Alignment was generated by using the Pileup program of Genetics Computer Group Sequence Analysis Software. Boldfaced/italicized columns identify acidic residues invariant among species. Letter "c" and "m" specify cytosolic and mitochondria isoforms, respectively. Numbers appearing above the sequence alignment correspond to the sequence assignments in the chicken cytosolic HMG-CoA synthase. Sequences from the following organisms and Accession Numbers are included: *Methanobacterium thermoautotrophicum*, AE000857; *Borrelia burgdorferi*, BB0683; *Schizosaccharomyces pombe*, U32187; *Saccharomyces cerevisiae*, P54839; *Caenorhabditis elegans*, P54871; *Arabidopsis thaliana*, X83882; *Pinus sylvestris*, X96386; m*Mus musculus*, P54869; m*Rattus norvegicus*, P22791; m*Sus scrofa*, U90884; m*Homo sapiens*, P54868; c1*Blattella germanica*, P54961; c2*Blattella germanica*, P54870; c*Gallus gallus*, P23228; c*Rattus norvegicus*, P17425; c*Cricetulus griseus*, P13704; c*Homo sapiens*, X66435.

(D99) is invariant in the eukaryotic and *B. burgdorferi* proteins while the sequence of the *M. thermoautotrophicum* protein exhibits a gap in this region of the alignment (Figure 2). Although it seemed likely that these six residues represent optimal targets for functional investigation by site-directed mutagenesis, the lack of demonstrated function for the prokaryotic proteins prompted us to evaluate all 11 residues that are invariant in an alignment of the more homologous eukaryotic proteins.

Expression, Isolation, and Preliminary Characterization of Mutant HMG-CoA Synthases. Expression constructs that encode replacement of each of 11 acidic residues with alanine were initially prepared and used to produce mutant HMG-CoA synthases. In those cases (E37A, E63A, and D64A) where alanine replacement destabilized protein structure and resulted in expression of insoluble enzyme, expression constructs that encode more conservative substitution of asparagine/glutamine for aspartate/glutamate were prepared and used to recover soluble enzyme. All soluble mutant enzymes with the exception of E37Q, E63Q, and D64N were very stable, allowing isolation to a high degree of homogeneity (>95%). The level of homogeneity of the three stable mutants (D99A, D159A, and D203A) for which detailed characterization is presented is comparable to that achieved with wild-type enzyme. Limited stability of E37Q, E63Q, and D64N prompted isolation of these proteins to enrichments of 52, 63, and 76%, respectively, based on SDS gel densitometry estimates; V_{max} estimates for these mutants are corrected accordingly.

Each mutant was used for V_{max} and $K_{m\ acetyl-CoA}$ determinations (Table 1). For the partially purified mutants, there were minimal changes in K_m and only modest drops in V_{max} for E37Q and E63Q, suggesting that E37 and E63 influence protein structure but are not crucial to HMG-CoA synthase's catalytic function. D64N exhibited a V_{max} decrease of 2 orders of magnitude, an observation compatible with a possible function for D64 in support of catalysis. However, the limited stability of the D64N mutant coupled with an effect on catalysis that is more modest in magnitude than results observed upon mutation of other acidic residues (vide infra) prompted us to focus effort on characterization of other targets. Highly purified preparations of E121A, D124A, D217A, and D282A were stable and exhibited V_{max} and $K_{m\ acetyl-CoA}$ values that differed less than 3-fold from estimates for wild-type enzyme; these mutants were not characterized in more detail. In contrast, highly purified preparations of the stable mutants E95A, D99A, D159A, and D203A exhibited decreases in V_{max} of >5, 2, 3, and 4 orders of magnitude, respectively. The large impact of substitution of E95 on catalytic efficiency prompted a separately published characterization of this mutant, which has suggested

Table 1: Comparison between the Catalytic Efficiencies of Wild-Type and Mutant HMG-CoA Synthases

enzyme	V_{max} (U/mg)[a]	$K_{m\ acetyl-CoA}$ (μM)[b]
wild type	4.40 ± 0.39	290 ± 22
E37Q[d]	0.125 ± 0.003	354 ± 38
E63Q[d]	3.02 ± 0.04	189 ± 10
D64N[d]	0.032 ± 0.001	118 ± 9
E95A	<0.00002	ND[c]
D99A	0.030 ± 0.002	207 ± 18
E121A	1.97 ± 0.11	372 ± 44
D124A	2.25 ± 0.20	677 ± 106
D159A	0.0033 ± 0.0001	7.8 ± 0.5
D203A	0.00036 ± 0.00003	37 ± 8
D217A	2.13 ± 0.09	319 ± 30
D282A	2.55 ± 0.07	358 ± 19

[a] V_{max} of wild-type HMG-CoA synthase and those mutants exhibiting no more than a 100-fold diminution in activity were measured using the spectrophotometric assay. Mutants exhibiting larger reductions in activity were measured using the radioisotopic assay. [b] $K_{m\ acecyl-CoA}$ is an apparent value, determined in the presence of 20 μM acetoacetyl-CoA. [c] Not determined; activity too low to measure accurately. [d] All enzymes isolated are soluble, stable, and >95% homogeneous except for E37Q, E63Q, and D64N. Partial stability of these three mutant enzymes limited purification to 52%, 63%, and 76%, respectively, based on densitometry estimate. V_{max} estimates for these mutants are corrected accordingly.

Table 2: Kinetic Parameters and Binding Properties of HMG-CoA Synthase Mutants

parameter	wild type	D99A	D159A	D203A
V_{max}, overall reaction (U/mg)	4.40 ± 0.39	0.030 ± 0.002	0.0033 ± 0.0001	0.00036 ± 0.00003
$K_{m\ acetyl-CoA}$ (μM)[a]	290 ± 22	207 ± 32	7.8 ± 0.5	37 ± 8
$K_{m\ acetoacetyl-CoA}$ (μM)[b]	1.19 ± 0.12	66 ± 17	49 ± 6	ND [f]
R·CoA binding stoichiometry[c]	0.9	1.0	1.0	0.95
K_d for R·CoA (μM)[c]	102 ± 20	233 ± 42	155 ± 33	583 ± 140
Ac-CoA binding stoichiometry (incubation time <5 s)[d]	1.1 ± 0.2	0.24 ± 0.09	0.43 ± 0.22	0.55 ± 0.20
stoichiometry of initial covalent acetylation (incubation time <5 s)[e]	0.63 ± 0.06	0.04 ± 0.05	0.09 ± 0.06	0.03 ± 0.06
end point acetylation stoichiometry[e]	0.62 ± 0.03	0.64 ± 0.03	0.57 ± 0.03	0.54 ± 0.02

[a] $K_{m\ AcCoA}$ is an apparent value, determined in the presence of acetoacetyl-CoA. [b] $K_{m\ AcAcCoA}$ is an apparent value, determined in the presence of 200 μM acetyl-CoA. [c] Dissociation constant and binding stoichiometry for R·CoA were calculated for wild-type and mutant enzymes by Scatchard analysis as described in Methods. Stoichiometry is calculated based on a 57.6-kDa subunit. [d] Determined by rapid centrifugal gel filtration after incubation of enzyme for less than 5 s with 1 mM [^{14}C]acetyl-CoA. [e] Determined by TCA precipitation after incubation of enzyme with saturating levels of [^{14}C]acetyl-CoA. [f] Not determined; activity too low to measure accurately.

a function for this residue in general acid/base catalysis (*24*). For the other mutants that display substantial catalytic defects, the $K_{m\ acetyl-CoA}$ value for D99A is little different from that exhibited by wild-type enzyme. Estimates for D159A and D203A are lower (tighter) than wild-type values (Table 1), indicating that impaired saturation by substrate acetyl-CoA does not account for depressed catalytic activity. On the basis of this initial survey of mutants in which acidic residues have been individually replaced, D99A, D159A, and D203A mutant proteins were selected for more detailed characterization.

Characterization of Catalytically Deficient HMG-CoA Synthase Mutants. For D99A and D159A, the levels of residual activity are sufficiently high for measurement of an apparent K_m for the second substrate, acetoacetyl-CoA (Table 2). The ~50-fold numerical increases in this parameter certainly represent a significant contrast with wild-type enzyme, but such changes remain secondary to the major effect on catalytic efficiency. In the case of D203A, the modest residual activity complicates estimate of a K_m for acetoacetyl-CoA, underscoring the need for an independent method for comparison of mutant structure with that of wild-type enzyme. Previous characterization of HMG-CoA synthase mutants (*12*, *13*) has benefitted from the availability of the spin-labeled analogue, R·CoA, which binds to the acetyl-CoA site as a competitive inhibitor (*17*) and produces an ESR signal indicating strong immobilization of the probe. Additionally, the disappearance of signal due to free spin-label facilitates quantitation of binding; Scatchard analysis allows these data to be straightforwardly analyzed to produce binding stoichiometry and K_d estimates for the analogue (Figure 3 shows a representative Scatchard plot of R·CoA binding to D99A). R·CoA binding studies were performed for all of the catalytically deficient mutants; Scatchard parameters are summarized in Table 2. In all cases, binding stoichiometry (calculated on the basis of a 57.6-kDa subunit) agrees well with the value measured for wild-type enzyme, indicating that each mutant contains a full complement of functional acyl-CoA sites. K_d for the spin-labeled probe varies by no more than 6-fold from the estimate for wild-type enzyme, further arguing that active site structure is not seriously altered. Finally, by analysis of the spectral features of the bound spin probe, the rotational dynamics of the heterocyclic acyl group can be evaluated. This group remains substantially immobilized when R·CoA binds to each mutant. Estimates of correlation times ($\tau_c = 35 \pm 4$ ns) compare well with the 35-ns value reported for wild-type enzyme (*12*).

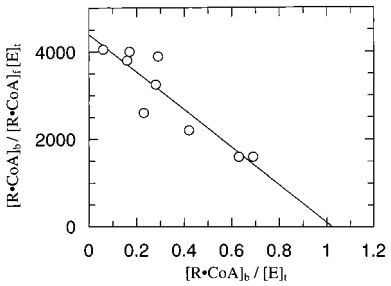

FIGURE 3: Scatchard plot of R·CoA binding to D99A HMG-CoA synthase. Data were obtained by mixing various amounts of D99A synthase (10−600 μM) with a fixed concentration of R·CoA (25 μM). The amount of free ($[R\cdot CoA]_f$) and bound ($[R\cdot CoA]_b$) spin label were determined as indicated in methods. The data were normalized with respect to enzyme concentration ([E]).

These observations indicate that no mutant exhibits significant alteration of secondary or tertiary structure that would increase local mobility, detectable as more rapid tumbling of the heterocyclic reporter group. It seems quite probable that, if the active site binding of the acyl-CoA substrate analogue remains substantially unchanged in these mutants, the overall tertiary structure of these proteins remains intact. Thus, the issue of why catalytic efficiency is significantly impaired in these mutants needs to be addressed.

Acetyl-S-Enzyme Reaction Intermediate Formation by Catalytically Deficient HMG-CoA Synthase Mutants. Acetyl-CoA binding stoichiometries have been measured for D99A, D159A, and D203A by performing centrifugal gel filtration of enzyme-acetyl-CoA mixtures (Table 2). As previously demonstrated for wild-type enzyme (*12*, *18*), such stoichiometries include a component from a noncovalent Michaelis complex (E∗Ac-CoA) as well as from the covalent acetyl-S-enzyme species. After short incubations sufficient for full loading of wild-type enzyme, each of the D99A, D159A, and D203A mutants exhibit substantially lower binding stoichiometries. Thus, it seemed important to also evaluate the level and the rate at which formation of the covalent reaction intermediate, acetyl-S-enzyme, occurs.

Upon brief incubation with acetyl-CoA, wild-type enzyme is efficiently covalently acetylated, while D99A, D159A, and D203A mutants exhibit markedly diminished covalent acetylation stoichiometry (Table 2), suggesting that this early step in the reaction sequence is defective. When incubation of enzyme with acetyl-CoA is allowed to proceed for an extended time period and the level of covalent acetyl-S-enzyme adduct is periodically evaluated by TCA precipitation of representative aliquots of the incubation mixture, it is clear

Table 3: Partial Reactions Catalyzed by Wild-Type HMG-CoA Synthase and Mutants Impaired in Acetyl-S-Enzyme Formation

parameter	wild type	D99A	D159A	D203A
V_{max} (U/mg) acetyl-S-enzyme formation	1.59 ± 0.16	0.0025 ± 0.0003	0.0026 ± 0.00005	0.0016 ± 0.00007
$K_{m\ acetyl-CoA}$ (μM) acetyl-S-enzyme formation	22.7 ± 8.3	623 ± 174	8.1 ± 1.0	448 ± 57
V_{max} (U/mg) acetyl-CoA hydrolysis[a]	0.030 ± 0.005	≅0.0007	0.0026 ± 0.00005	≅0.0005
$K_{m\ acetyl-CoA}$ (μM) acetyl-CoA hydrolysis	14 ± 2	ND[b]	33 ± 10	ND[b]
k_{cat} (s^{-1}) acetyl-S-enzyme hydrolysis[c]	0.0036 ± 0.0005	0.0003 ± 0.00006	0.0008 ± 0.00005	0.0005 ± 0.00006

[a] Steady-state measurement involves measurement of [^{14}C]acetyl-CoA depletion by conversion of residual substrate (in an aliquot of reaction mix) to acid stable [^{14}C]citrate using excess citrate synthase and oxaloactate. [b] Not determined; K_m determination precluded by low activity of this mutant. [c] After rapid centrifugal gel filtration isolation of reaction intermediate, residual level is measured over time as ^{14}C radioactivity in TCA-precipitated aliquots of the sample.

that D99A, D159A, and D203A can certainly form covalent acyl-S-enzyme at levels approaching wild-type synthase (Table 2). More extensive kinetic studies of acetyl-S-enzyme formation were conducted (pH 7.0; 22 °C) using a rapid mix/quench apparatus (25−160 ms time scale) for measurements on wild-type enzyme, while manual techniques sufficed for rate measurements on D99A, D159A, and D203A, which display ~3 orders of magnitude decreases in acetylation rate (Table 3). To allow comparison with activity measurements (pH 8.2; 30 °C) for the overall condensation reaction that produces HMG-CoA, the reported acetylation rates must be increased by ≥9-fold to compensate for differences in pH and temperature. For wild-type enzyme and also for D99A synthase, such corrections produce a rate for acetyl-S-enzyme formation which is close to that measured for the overall reaction, suggesting that acetylation approaches rate-limiting status. In the case of wild-type enzyme, such an observation would explain the failure to detect any substantial kinetic isotope effect on k_{cat} when deuterated acetyl-CoA is used in assays of HMG-CoA production (H. Miziorko, unpublished observations). Comparable correction of the acetylation rates for D159A and D203A enzymes produces values well in excess of the rates of their respective condensation reactions (Table 2), suggesting that mutations of these residues influence not only acetylation but also other reaction steps.

Single Turnover Reactions Catalyzed by Slow Acetylating Mutant HMG-CoA Synthases. Another approach to identifying which of the three steps in the reaction pathway is impaired by mutation involves measurement of the efficiency of single condensation reaction turnover. This is accomplished by preincubation of substrate quantities of enzyme with [^{14}C]acetyl-CoA, forming stoichiometric levels of [^{14}C]acetyl-S-enzyme species. For wild-type enzyme, a 5-s preincubation with substrate is sufficient for optimal formation of acetyl-S-enzyme (stoichiometry ≥0.5/active site). The slow acetylating mutant enzymes require longer preincubations with [^{14}C]acetyl-CoA to reach comparable reaction intermediate stoichiometry (D99A, 22 min; D159A, 18 min; D203A, 35 min). The reaction mixture is passed through a centrifugal gel filtration column to remove unbound [^{14}C]acetyl-CoA; the [^{14}C]acetyl-S-enzyme intermediate is isolated and combined with an excess of the unlabeled second substrate, acetoacetyl-CoA; and aliquots are either subjected to TCA precipitation (to monitor radiolabeled acyl-S-enzyme intermediates) or taken to dryness from 6 N HCl at 95 °C to detect the radiolabeled condensation intermediate (Enz-S-HMG-CoA) or product (free HMG-CoA). As expected, when this reaction is performed with wild-type enzyme, there is an efficient, rapid turnover (Figure 4) of [^{14}C]acetyl-S-enzyme (stoichiometry ≅ 0.6/active site) into the acid stable (6 N HCl) condensation product, [^{14}C]HMG-CoA (stoichiometry ≅ 0.6/active site). At time ≅ 0 (elapsed time required for fastest possible manual addition of second substrate, followed by withdrawal of paired aliquots into TCA or HCl), greater than 80% of the acetyl group has condensed with the second substrate to form HMG-CoA, which has been released from enzyme since the stoichiometry of radiolabeled acyl-S-enzyme intermediate is less than 0.1 per active site (Figure 4). After 2 min, all residual [^{14}C]acetyl moieties have been converted to free [^{14}C]HMG-CoA. The efficiency of single condensation turnover for the three mutants differs somewhat, with D99A and D159A both reaching completion in <4 min while D203A requires >10 min. The data for all three mutants clearly illustrate that, once the major defect in the acetylation step has been compensated for by a longer incubation period with acetyl-CoA, the remaining reaction steps (condensation and product release) are less profoundly affected by the mutation.

Enzyme-Catalyzed Steady-State Hydrolysis of Acetyl-CoA. In the absence of a suitable acetyl group acceptor, such as acetoacetyl-CoA or CoASH, HMG-CoA synthase catalyzes the slow abortive hydrolysis of acetyl-CoA to form acetate and CoA. Under steady-state conditions, this hydrolysis reaction is monitored by following the disappearance of [^{14}C]acetyl-CoA through its conversion to an acid-stable form ([^{14}C]citrate) in the presence of excess citrate synthase and oxaloacetate (*19*). D159A synthase catalyzes acetyl-CoA hydrolysis with a 10-fold diminution in catalytic efficiency and only a modest (2.5-fold) increase in the $K_{m\ acetyl-CoA}$. For the other two mutant synthases (D99A and D203A), the rate of hydrolysis is depressed by approximately 50-fold [$\sim 0.0005-0.0007$ U/mg^{-1} (Table 3)]. This low residual activity precluded measurements of rates under suboptimal (low substrate) conditions. Thus, estimates of K_m for acetyl-CoA cannot be determined. The rate differences between the three mutants are smaller than the contrasts in their rate of overall reaction catalysis. Since these steady-state hydrolysis measurements are performed in the presence of high levels of acetyl-CoA with accumulation of free CoASH, it seemed that evaluation of the intrinsic ability of these mutant enzymes to catalyze reaction intermediate hydrolysis would be refined by directly monitoring turnover of that isolated species.

Hydrolysis of the Acetyl-S-Enzyme Reaction Intermediate. Acetyl-S-enzyme containing approximately 0.5 acetyl group/active site was prepared by the incubation of synthase enzyme with [^{14}C]acetyl-CoA and isolation by gel filtration as described in Methods. At various times, an aliquot of the acetyl-S-enzyme reaction mixture was precipitated with TCA, and the percent of covalently bound was determined. The

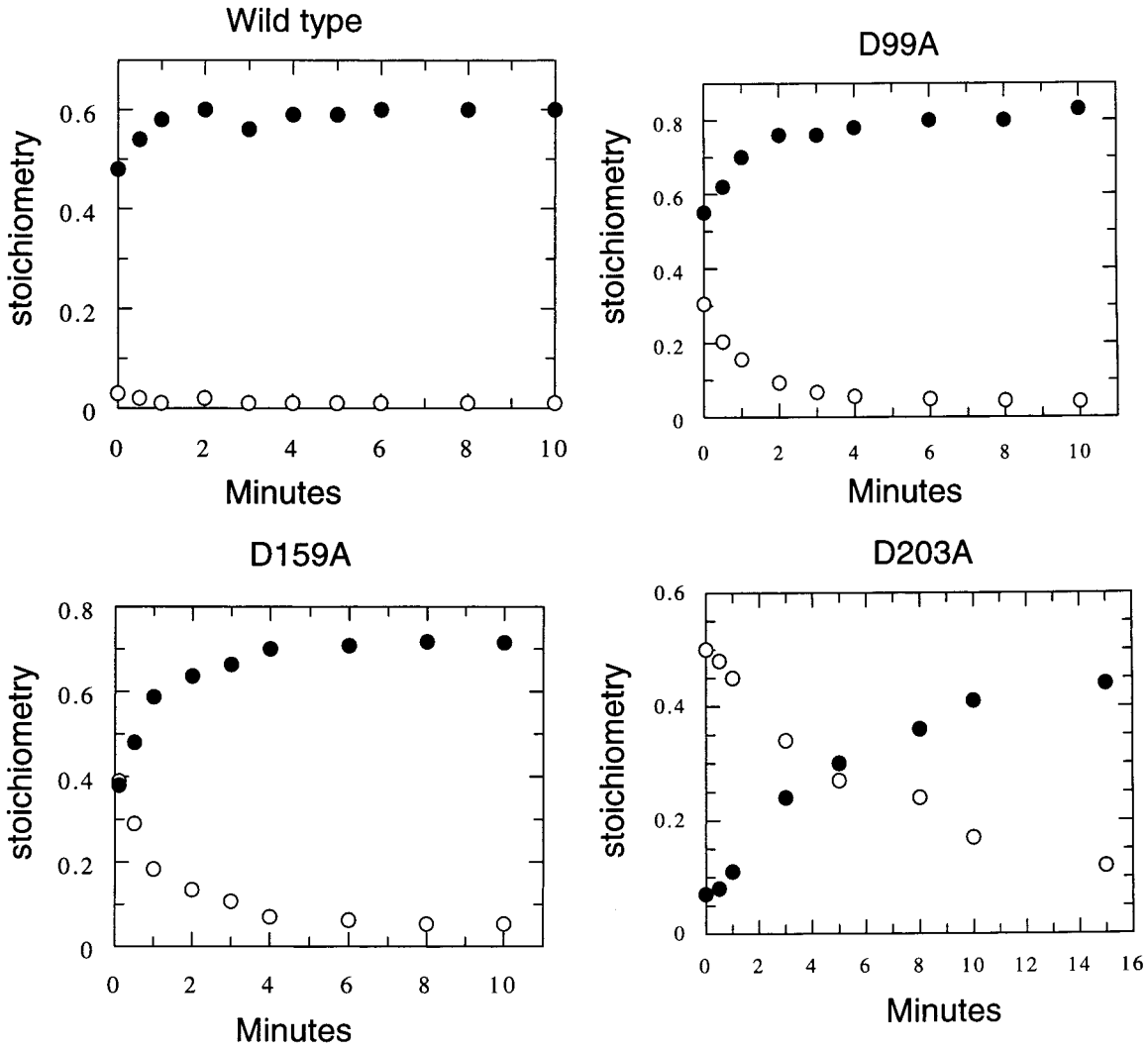

FIGURE 4: Single turnover condensation reaction of wild-type, D99A, D159A, and D203A HMG-CoA synthases. Each enzyme (25 μM) was incubated with saturating [1-^{14}C]acetyl-CoA (500−1000 μM; 12 000 dpm/nmol). Unbound acetyl-CoA was removed by centrifugal gel filtration. Excess unlabeled second substrate, acetoacetyl-CoA (10-fold molar excess), was added to the isolated acetyl-S-enzyme samples to drive the reaction to completion. The reactions mixtures were monitored over time for formation of the HMG-CoA condensation product, measured as acid stable (6 N HCl), TCA soluble radioactivity (●), as well as for the residual level of covalent acyl-enzyme intermediates, measured as TCA precipitable radioactivity (○).

release of ^{14}C from the enzyme follows first-order kinetics. For wild-type enzyme, the rate constant for acetyl-S-enzyme hydrolysis at pH 7.0 and 30 °C is 0.0036 s^{-1} (Table 3). This value closely approximates the reported acetyl-enzyme hydrolysis rate (0.0017 s^{-1}) obtained under the same conditions from tissue-isolated ox liver mitochondrial HMG-CoA synthase (*25*). In comparison to steady-state acetyl-CoA hydrolysis, acetyl-S-enzyme hydrolysis is approximately 10-fold slower. Under steady-state conditions, nucleotide that is present as the accumulating CoASH or as unreacted acetyl-CoA may occupy the nucleotide binding site, facilitating the hydrolytic release of the acetyl group from the acetyl-S-enzyme reaction intermediate.

Exchange of $H_2{}^{18}O$ Solvent with Acetyl-S-Enzyme. Recently, the ability of the thioester carbonyl oxygen of acetyl-S-enzyme to exchange with solvent oxygen was demonstrated (*26*) by an approach that involved the use of ^{13}C-enriched acetyl-CoA to form the reaction intermediate and ^{18}O-enriched solvent to allow detection of exchange as an upfield shift in the ^{13}C NMR peak assigned to the thioester carbonyl. Any observed solvent exchange demands the transient reversible formation of a diol-containing tetrahedral adduct. The formation of an acetyl-S-enzyme does not guarantee facile reversible formation/collapse of a diol-containing tetrahedral adduct. For example, the C378G mutant form of β-ketothiolase accumulates the acetyl-S-enzyme reaction intermediate (*27*) but fails to equilibrate ^{18}O solvent with the thioester carbonyl oxygen. Thus, the active site of wild-type HMG-CoA synthase contains residues that selectively support the reversible solvent addition/elimination reaction. The slow acetylation mutants were therefore tested to determine whether the functions that D99, D159, or D203 support in formation of acetyl-S-enzyme or other steps in the overall reaction were also important to formation/collapse of the diol-containing tetrahedral adduct.

The active site integrity of mutants D99A, D159A, and D203A is validated by their formation of [^{13}C]acetyl-S-enzyme intermediates, which exhibit substantial upfield NMR shifts for the C1 and C2 acetyl resonances that match those observed for wild-type enzyme (Figure 5). While any precise measurement of the kinetics of exchange is precluded by the extended time required to acquire a ^{13}C NMR spectrum,

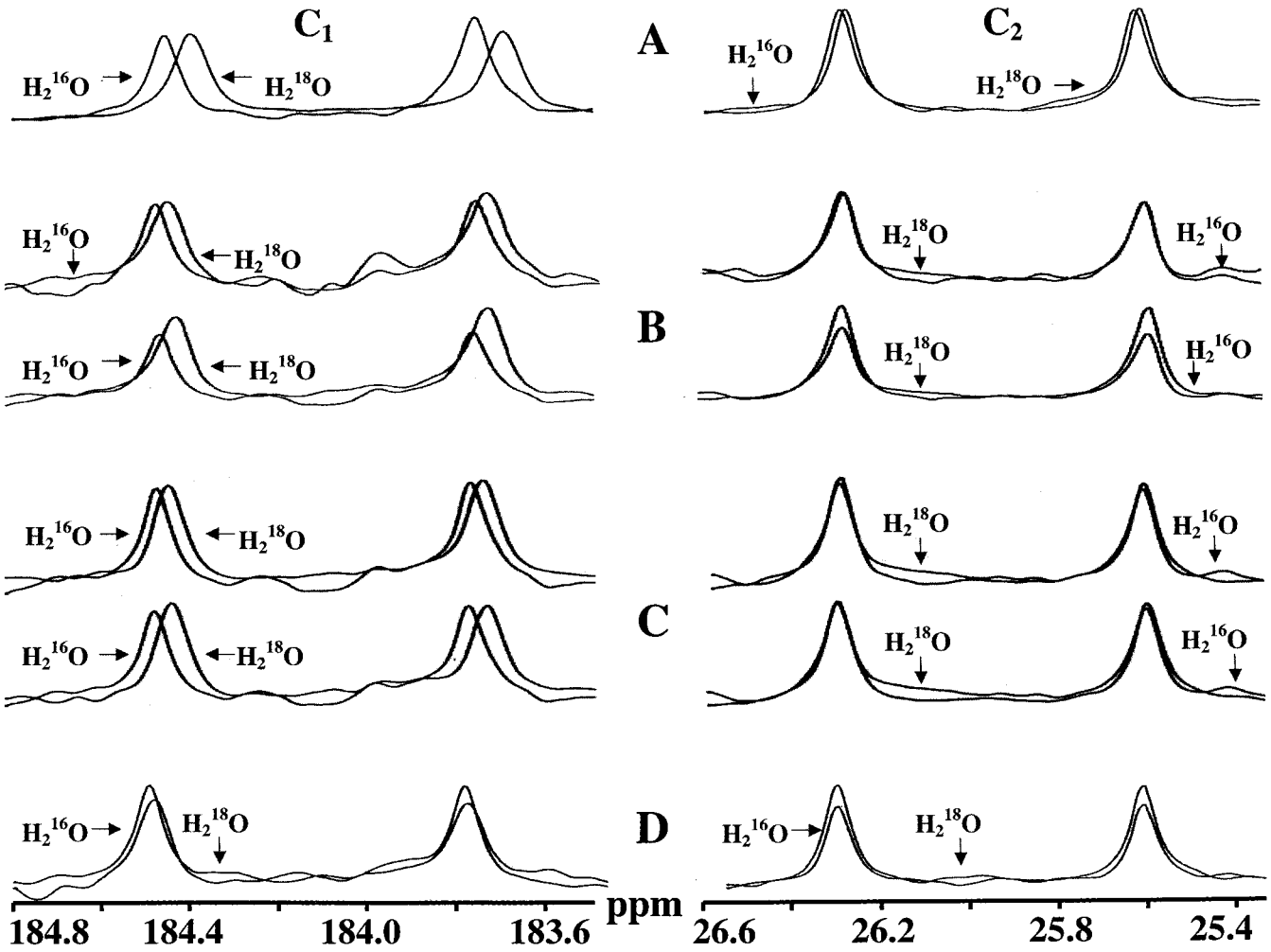

FIGURE 5: ^{18}O isotope shifts in ^{13}C NMR signal due to the thioester carbonyl of the [^{13}C]acetyl-S-enzyme reaction intermediate. Samples were prepared as described in Experimental Procedures and contained the following: (A) wild-type enzyme (1 mM) with [1,2-^{13}C]acetyl-CoA (2 mM) in $H_2{}^{18}O$ vs $H_2{}^{16}O$; (B) D159A (1 mM) with [1,2-^{13}C]acetyl-CoA (2 mM) in $H_2{}^{18}O$ vs $H_2{}^{16}O$; (C) D203A (1 mM) with [1,2-^{13}C]acetyl-CoA (2 mM) in $H_2{}^{18}O$ vs $H_2{}^{16}O$; (D) D99A (1 mM) with [1,2-^{13}C]acetyl-CoA (2 mM) in $H_2{}^{18}O$ vs $H_2{}^{16}O$. Left panels depict signals due to the C1 thioester carbonyl; right panels depict signals due to the C2 methyl group. The spectrum for sample A was measured after 3 h. The spectra for samples B and C were measured after 5 and 10 h. The spectrum for sample D was measured after 10 h.

Figure 5 demonstrates that this approach does indeed discriminate between the functions of these residues. The ability of wild-type HMG-CoA synthase's acetyl-S-enzyme to reversibly form/collapse a tetrahedral intermediate is demonstrated by reconstituting freeze-dried enzyme in $H_2{}^{18}O$ vs $H_2{}^{16}O$ and adding [1,2-^{13}C]acetyl-CoA, appropriately dissolved in $H_2{}^{18}O$ or $H_2{}^{16}O$ (Figure 5A). Use of doubly labeled [l,2-^{13}C]acetyl-CoA affords an internal control, since the 26 ppm C2 methyl peak can be observed in $H_2{}^{18}O$ and $H_2{}^{16}O$ experiments to verify that no significant upfield shifts are observed for this carbon, which contains no C−O bond. For the resonance corresponding to the C1 thioester carbon of acetyl-S-enzyme (184.3 ppm), the substitution of $H_2{}^{18}O$ for $H_2{}^{16}O$ resulted in an upfield shift of 0.055 ± 0.005 ppm, as measured after 3 h of signal accumulation. The magnitude of the shift did not increase upon further signal accumulation. In contrast to the observations on C1, the substitution of $H_2{}^{18}O$ for $H_2{}^{16}O$ had very little effect on the resonance corresponding to the C2 methyl carbon (26 ppm), as expected. After 3 h of signal accumulation the observed upfield shift was 0.009 ± 0.002 ppm (Figure 5A), a value that remained unchanged upon further signal accumulation and reflects experimental error.

Reaction of D159A and D203A HMG-CoA synthases ([enzyme sites] = 1 mM in each sample) with [1,2-^{13}C]-acetyl-CoA (2 mM) in $H_2{}^{18}O$ vs $H_2{}^{16}O$ resulted in the ^{13}C NMR spectra shown in Figure 5B,C. For the resonance corresponding to the C1 thioester carbonyl (184.3 ppm) of acetyl-S-D159A and acetyl-S-D203A, the substitution of $H_2{}^{18}O$ for $H_2{}^{16}O$ resulted in upfield shifts of 0.027 ± 0.004 ppm and 0.020 ± 0.003, respectively, measured after 5 h of signal accumulation. The magnitude of the shifts increased to 0.040 ± 0.004 and 0.035 ± 0.003, respectively, after 10 h of signal accumulation (Table 4) and remained unchanged upon further signal accumulation. The substitution of $H_2{}^{18}O$ for $H_2{}^{16}O$ had a minimal effect on the resonances corresponding to the C2 methyl carbon (26 ppm) of acetyl-S-enzyme species produced using D159A and D203A. After 5 and 10 h of signal accumulation, both observed upfield shifts were 0.003 ± 0.001 ppm; these values remained unchanged upon further signal accumulation and reflect the magnitude of experimental error in these experiments.

Reaction of D99A HMG-CoA synthase (1 mM) with [1,2-^{13}C]acetyl-CoA (2 mM) in $H_2{}^{18}O$ vs $H_2{}^{16}O$ resulted in the ^{13}C NMR spectra shown in Figure 5D. In contrast with the results obtained using wild-type, D159A, and D203A

Table 4: Summary of ^{18}O-Induced Isotope Shifts of the ^{13}C Resonances of Ac-CoA, Acetyl-S-Wild-Type, Acetyl-S-D159A, Acetyl-S-D203A, and Acetyl-S-D99A Synthase Reaction Intermediates

sample		line width (Hz)	$\Delta[\delta_{(H_2{}^{16}O)}-\delta_{(H_2{}^{18}O)}]^a$ (ppm)
Ac-CoA in buffer	C1	7.9	0.005 ± 0.001
	C2	6.1	0.006 ± 0.001
acetyl-S-WT synthase	C1	17.0	0.055 ± 0.005
	C2	15.8	0.009 ± 0.002
acetyl-S-D159A synthase	C1	16.9	$0.027 \pm 0.004 \rightleftharpoons 0.040 \pm 0.004$
	C2	16.2	$0.003 \pm 0.001 \rightleftharpoons 0.003 \pm 0.001$
acetyl-S-D203A synthase	C1	16.9	$0.020 \pm 0.003 \rightleftharpoons 0.035 \pm 0.003$
	C2	16.6	$0.003 \pm 0.001 \rightleftharpoons 0.003 \pm 0.001$
acetyl-S-D99A synthase	C1	16.2	0.010 ± 0.002
	C2	16.4	0.002 ± 0.001

[a] Standard error for differential isotope shift values was calculated from two independently exchanged and consecutively run samples.

enzymes, the substitution of $H_2{}^{18}O$ for $H_2{}^{16}O$ resulted in a minimal upfield shift of 0.010 ± 0.002 ppm for the resonance corresponding to the C1 thioester carbonyl (184.3 ppm) of acetyl-S-D99A, measured after 10 h of signal accumulation. The magnitude of the shift (Table 4) remained unchanged upon further signal accumuation. The substitution of $H_2{}^{18}O$ for $H_2{}^{16}O$ had a negligible effect on the resonance corresponding to the C2 methyl carbon (26 ppm) of acetyl-S-D99A. After 10 h of signal accumulation, the observed upfield shift was 0.002 ± 0.001 ppm, a value that remained unchanged upon further signal accumulation. While these three mutants vary in kinetics of ^{18}O exchange, they all exhibit reduced exchange rates, as expected if they are impaired in the acetyl-S-enzyme formation step, which is a prerequisite to hydration and formation of the diol-containing tetrahedral adduct required to account for the observed solvent exchange reaction.

DISCUSSION

The functional survey of invariant acidic residues successfully identified several residues which contain side chains that influence catalytic efficiency (Table 1). Before attributing mechanistic significance to such results, it is crucial to evaluate the structural integrity of the mutants in which these acidic groups have been replaced. Certainly in the case of D99A, D159A, and D203A proteins, their ability to bind a competitive inhibitor (Table 2) with affinity and stoichiometry similar to that observed for wild-type HMG-CoA synthase argues that these proteins retain largely unperturbed tertiary structure. An explanation of the basis for the 10^2-10^4-fold diminution in catalytic efficiency thus becomes the next issue to be addressed. In the case of HMG-CoA synthase, consideration of the overall reaction as a three-step process is useful since it prompts tests that discriminate between whether the impairment in catalysis involves a precondensation, condensation, or product release (hydrolysis) step. For D99A, D159A, and D203A synthases, a variety of partial reactions (Table 3) indicate that, while these mutants vary somewhat in their intrinsic ability to catalyze C−C bond formation, most of the observed diminution in catalytic efficiency is attributable to retarded kinetics of production of the acetyl-S-enzyme reaction intermediate.

The observation that mutations which delete each of three different acidic residues all affect formation of the same

Scheme 2

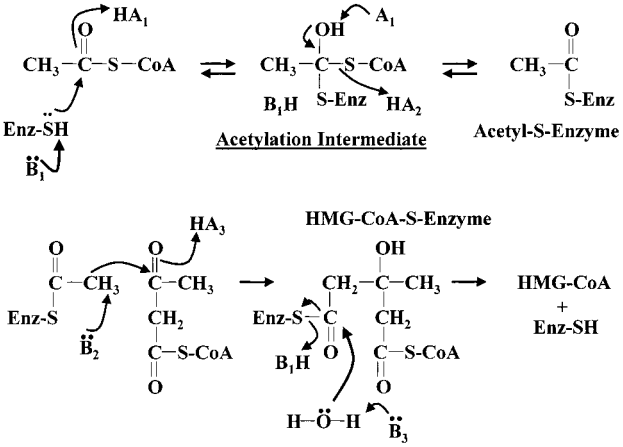

reaction intermediate suggests that this step involves more than just unassisted attack of the thiolate of C129 on the thioester carbonyl of substrate acetyl-CoA (as depicted in Scheme 1, reaction 1). The formation and collapse of a tetrahedral intermediate on the pathway to acetyl-S-enzyme formation (Scheme 2) could require participation of several active site amino acids, accounting for results observed with D99, D159, and D203 mutants. While this intermediate has not been directly demonstrated, its existence seems quite plausible based on recent work (*26*) which has demonstrated that an analogous tetrahedral adduct participates in the related side reaction that accounts for acetyl-S-enzyme hydrolysis.

Formation of a tetrahedral intermediate on the pathway to acetyl-S-enzyme formation (Scheme 2) likely requires assistance in deprotonation of C129 to form a reactive thiolate species. The pH/rate profile for HMG-CoA synthase (*14*) indicates a pK_a of 8.6, a value attributable either to enolization of the second substrate, acetoacetyl-CoA, or to the side chain of an active site amino acid. Observations on a nonenolizable alternative second substrate (D. Vinarov, unpublished) indicate that a pH dependence persists, suggesting that the pK_a reflects ionization of an amino acid side chain. The observed pK_a value might suggest participation of a cysteine, but this would only be likely if the thiol-containing side chain were situated in a typical aqueous environment. In a low dielectric environment, cysteine's pK_a is elevated to pH $\geq$ 10 (*28*, *29*). In the case of the active site of HMG-CoA synthase, ^{13}C and ^1H NMR measurements have detected upfield shifts of signals due to carbon (*27*) and protons (*24*) of the acetyl group of the acetyl-S-enzyme intermediate; these shifts argue strongly for a low dielectric environment at the active site. This demands catalytic assistance in C129 deprotonation which, if eliminated, will result in a diminished rate of intermediate production.

A second requirement for an active site residue involves protonation of the thioester carbonyl to produce an alcohol substituent in the tetrahedral adduct (Scheme 2). This protonation is a transient modification that must be reversed in the process of directed collapse of the adduct to reform the thioester carbonyl of the acetyl-S-enzyme intermediate.

Finally, to support productive forward collapse of the tetrahedral adduct to produce reaction intermediate (Scheme 2) instead of backward collapse to reform substrate and free enzyme, there must be efficient expulsion of the $CoAS^-$

leaving group. There is ample bioorganic model work (*30*) to indicate that protonation of the thiolate is required to make this process efficient.

While the detailed chemistry outlined above provides possible functions that may require the participation of residues such as D99, D159, or D203 (or other active site residues), a question arises concerning whether the available data support assignment of precise roles to any of these amino acids. While no definitive assignments are currently possible, the data support reasonable postulates and formulation of a working model that seems consistent with all experimental observations. Any explanation must, of course, address the observations that, in comparison with wild-type synthase, all three variants are markedly diminished in efficiency of covalent intermediate formation. However, there is only a 2-fold difference between the three diminished rates of intermediate formation (Table 3), and a working model should also address the difference of 2 orders of magnitude between these three mutants' k_{cat} values for the overall production of HMG-CoA (Table 2).

In the case of D99, there seems to be little need to invoke participation in steps other than acetyl-S-enzyme formation. Comparison of the three mutants indicates that single condensation turnover for D99A most closely approaches the observations made with wild-type enzyme. Additionally, the rate of acetyl-S-enzyme formation approaches rate-limiting status in D99A's overall condensation reaction. The deficiency of D99A in catalysis of solvent oxygen exchange (Figure 5; Table 4) is interesting and invites speculation that the side chain could be involved in thioester carbonyl protonation steps common to tetrahedral adducts that are likely to form in both acetylation and hydrolysis. An alternative explanation derives from recent isotope effect results in bioorganic model reactions (*31*, *32*), which suggest that acyl transfer occurs via a "concerted" mechanism with attacking and leaving groups positioned on opposite faces of the carbonyl carbon. In order for the related process of solvent exchange into acetyl-S-enzyme to occur, wild-type HMG-CoA synthase may have to accommodate these spatial requirements. Failure of D99A to support solvent exchange (or efficient acetyl-S-enzyme formation) may simply derive from a perturbation of the precise active site positioning that is required. Since the diminution in overall reaction k_{cat} for D99A is quite modest (10^2 fold), an indirect role in positioning reactants or catalytic residues in the active site merits consideration.

The participation of D159 and D203 in additional steps in the reaction (Scheme 2) provides the simplest explanation for the larger magnitude of k_{cat} effects observed upon mutagenesis of these residues. The data for single condensation turnover (Figure 4) indicate lower efficiencies for D159A and D203A, supporting such a hypothesis. For example, any carboxyl group that supports C129 deprotonation during reaction intermediate formation might also support the terminal hydrolytic release of condensation product by protonation of C129's thiolate leaving group. Other steps in which these residues could be involved include the protonation step required to expedite expulsion of the CoA thiolate leaving group and forward collapse of a tetrahedral intermediate to form acetyl-S-enzyme (Scheme 2). An active site residue also is likely to support protonation of acetoacetyl-CoA's C3 keto group during condensation. Given the magnitude of diminution of k_{cat} for these mutants, a direct chemical role for D203 in one or more of these processes seems quite plausible. Mutation of D159 results in a less dramatic loss of function, so it remains possible that this residue may participate not directly in catalysis of a chemical step but instead to orient or alter the pK_a value of a side chain more directly involved in such chemistry.

ACKNOWLEDGMENT

Dr. Chakravarthy Narasimhan provided valuable assistance with the EPR measurements. These spin-labeling experiments were performed using the facilities of the National Biomedical ESR Center (supported by NIH Grant RR01008). Drs. Jennifer Runquist and Ila Misra provided valuable advice on strategy of construction of mutagenic expression plasmids.

REFERENCES

1. Miziorko, H. M., and Lane, M. D. (1977) *J. Biol. Chem. 252*, 1414−1420.
2. Clinkenbeard, K. D., Sugiyama, T., Reed, W. D., and Lane, M. D. (1975) *J. Biol. Chem. 250*, 3124−3135.
3. Reed, W. D., Clinkenbeard, K. D., and Lane, M. D. (1975) *J. Biol. Chem. 250*, 3117−3123.
4. Ayte, J., Gil-Gomez, G., Haro, D., Marrero, P. F., and Hegardt, F. G. (1990) *Proc. Natl. Acad. Sci. U.S.A. 87*, 3874−3878.
5. Kattar-Cooley, P. A., Wang, H. H. L., Mende-Mueller, L. M., and Miziorko, H. M. (1990) *Arch. Biochem. Biophys. 283*, 523−529.
6. Hegardt, F. G. (1999) *Biochem. J. 338*, 569−582.
7. Goldstein, J. L., and Brown, M. S. (1990) *Nature 343*, 425−430.
8. Lowe, D. M., and Tubbs, P. K. (1985) *Biochem. J. 232*, 37−42.
9. Thompson, G. N., Hsu, B. Y. L., Pitt, J. J., Treacy, E., and Stanley, C. A. (1997) *N. Engl. J. Med. 337*, 1203−1206.
10. Miziorko, H. M., and Behnke, C. E. (1985) *Biochemistry 24*, 3174−3179.
11. Miziorko, H. M., and Behnke, C. E. (1985) *J. Biol. Chem. 260*, 13513−13516.
12. Misra, I., Narasimhan, C., and Miziorko, H. M. (1993) *J. Biol. Chem. 268*, 12129−12135.
13. Misra, I., and Miziorko, H. M. (1996) *Biochemistry 35*, 9610−9616.
14. Misra, I., Charlier, H. A., and Miziorko, H. M. (1995) *Biochim. Biophys. Acta 1247*, 253−269.
15. Ho, S. N., Hunt, H. D., Horton, R. M., Pullen, J. K., and Pease, L. R. (1989) *Gene 77*, 51−59.
16. Bradford, M. M. (1976) *Anal. Biochem. 72*, 248−254.
17. Miziorko, H. M., Lane, M. D., and Weidman, S. W. (1979) *Biochemistry 18*, 399−403.
18. Vollmer, S., Mende-Mueller, L. M., and Miziorko, H. M. (1988) *Biochemistry 27*, 4288−4292.
19. Miziorko, H. M., Clinkenbeard, K. D., Reed, W. D., and Lane, M. D. (1975) *J. Biol. Chem. 250*, 5768−5773.
20. Means G. E., and Feeney R. E. (1971) *Chemical Modification of Proteins*, Holden-Day Inc., San Francisco, CA.
21. Rokosz, L. L., Boulton, D. A., Butkiewicz, E. A., Sanyal, G., Cueto, M. A., Lachance, P. A., and Hermes, J. D. (1994) *Arch. Biochem. Biophys. 312*, 1−13.
22. Fraser, C. M., et al. (1997) *Nature 390*, 580−586.
23. Smith, D. R., et al. (1997) *J. Bacteriol. 179*, 7135−7155.
24. Chun, K. Y., Vinarov, D. A., Zajicek, J., and Miziorko, H. M. (2000) *J. Biol. Chem. 275*, 17946−17953.
25. Lowe, D. M., and Tubbs, P. K. (1985) *Biochem. J. 227*, 601−607.
26. Vinarov, D. A., and Miziorko, H. M. (2000) *Biochemistry 39*, 3360−3368.

27. Vinarov, D. A., Narasimhan, C., and Miziorko, H. M. (1999) *J. Am. Chem. Soc. 121*, 270−271.
28. Dyson, H. J., Jeng, M. F., Tennant, L. L., Slaby, I., Lindell, M., Cui, D. S., Kuprin, S., and Holmgren, A. (1997) *Biochemistry 36*, 2622−2636.
29. Chivers, P. T., Prehoda, K. E., Volkman, B. F., Kim, B. M., Markley, J. L., and Raines, R. T. (1997) *Biochemistry 36*, 14985−14991.
30. Gilbert, H. F., and Jencks, W. P. (1977) *J. Am. Chem. Soc. 99*, 7931−7947.
31. Hengge, A. C., and Hess, R. A. (1994) *J. Am. Chem. Soc. 116*, 11256−11263.
32. Hess, R. A., Hengge, A. C., and Cleland, W. W. (1998) *J. Am. Chem. Soc. 120*, 2703−2709.

BI001805M